

Chaos in the Stadium Quantum Billiards

Syne O. Salem

Physics Department, The College of Wooster, Wooster, Ohio 44691, USA

(Dated: December 15, 2011)

An expansion method was used to write a MATHEMATICA program to compute the energy levels and eigenfunctions of a 2-D quantum billiard system with arbitrary shape and dirichlet boundary conditions. One integrable system, the full circle, and one non-integrable system, the stadium, were examined. Chaotic properties were sought in nearest-neighbor energy level spacing distributions (NND). It was observed that the classically non-chaotic Poisson function seemed to fit the circle's NND better, while the classically chaotic Gaussian Orthogonal Ensemble function the stadium better. A detailed explanation of the theory and algorithm are provided, although a more rigorous energy-level analysis is desirable.

PACS numbers: 87.10.+e, 05.45.-a, 87.19.Rr

I. INTRODUCTION

Classically, the billiard problem involves finding the motion of a free particle (a "billiard") in a closed geometry with elastic boundaries. The particle moves about the region with conserved energy. Given certain geometries and initial conditions, the billiard could display periodic or chaotic motion about the region. The problem has inspired numerous computer simulations and variants that demonstrate certain interesting properties of the arrangement. Earliest uses of billiard arrangements include the kinetic theory of gases, which was the launching point for both thermodynamics and statistical mechanics [1]. One way the problem can be studied is from a dynamical standpoint, by considering the way a system evolves over time. For classical billiards this can involve examining the actual trajectories of the billiards in certain geometries. Another option is to study a particular system with ergodic theory, which uses a more statistical and qualitative method to study systems. A goal of studying these systems can be finding chaotic trajectories, which implies extreme sensitivity to initial conditions and aperiodicity.

The quantum equivalent of the chaotic billiard problem must be approached differently because a quantum particle in a potential well is not clearly analogous to classical billiards. Instead of being determined by time sensitive trajectories and initial conditions, the boundary conditions alone determine whether a quantum billiard is chaotic. Energy levels of the solutions to the time-independent Schrodinger wave equation (TISWE) for simple geometries are usually spaced in particularly ordered ways. The quantum simple-harmonic oscillator has evenly spaced energy levels, while the infinite potential well has energy levels E_n that are separated by n^2 . By examining the probability of finding an energy level in the area ds about a particular energy level E , we can find distributions that are characteristic of classically chaotic systems. There are, of course, other ways that quantum billiards have been used to study correlations between chaos in classical and quantum systems. For example, it has been found that resonance spectrum in quantum chaotic systems bears many similarities to the classical

Ruelle-Pollicott resonances [2].

Not only theoretically interesting, the quantum billiard problem has several applications, especially in nanotechnology. Electrons in nanodevices are often confined to two spatial dimensions, and the billiard problem can adequately represent their ballistic motion. Quantum billiards have also recently been led to experimental recreation by a variety of techniques including electrical resonance circuits [3] and microwave cavities [4].

II. THE EXPANSION METHOD

To find solutions to a 2-D quantum billiard of arbitrary shape, I employ a simple expansion method developed by Kaufman, Kosztin, and Schulten [5]. The time-independent Schrodinger wave equation is

$$\hat{H}\psi_n(\mathbf{r}) = [-\frac{\hbar^2}{2M}\nabla^2 + V(\mathbf{r})]\psi_n(\mathbf{r}) = E_n\psi_n(\mathbf{r}). \quad (1)$$

We are interested in solving this for \mathbf{r} being part of some arbitrary region Γ , where

$$V(\mathbf{r}) = \begin{cases} 0 & \text{if } \mathbf{r} \in \Gamma \\ \infty & \text{if } \mathbf{r} \notin \Gamma \end{cases}. \quad (2)$$

To handle this, we introduce a rectangular region Γ' that encloses the region Γ , with a potential V_0 , high enough that the wavefunction will essentially be zero in it. Our new total potential is then

$$V'(\mathbf{r}) = \begin{cases} 0 & \text{if } \mathbf{r} \in \Gamma \\ V_0 & \text{if } \mathbf{r} \in \Gamma' \\ \infty & \text{if } \mathbf{r} \notin \Gamma \cup \Gamma' \end{cases}. \quad (3)$$

Figure 1 shows the total region in consideration, with a_1 and a_2 designating the lengths of the enclosing rectangle Γ' . Because the solutions to the Schrodinger wave equation are well known for a 2-D rectangular infinite potential well, we can describe the wavefunction in this

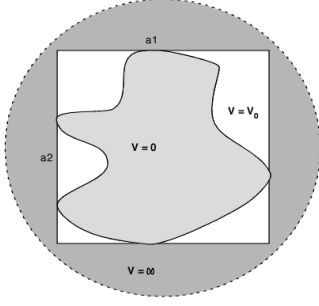


FIG. 1: The arbitrary region of interest Γ has no potential, while the rectangle that encloses it (of dimensions a_1 and a_2), Γ' , has a potential equal to V_0 . The potential is infinite elsewhere.

region with a convenient expansion:

$$\psi_n(\mathbf{r}) = \sum_m c_m \phi_m(\mathbf{r}), \quad (4)$$

where c_m are expansion coefficients and $\phi_m(\mathbf{r})$ are the eigenfunctions of a particle in the rectangular square well. Those eigenfunctions are given by

$$\phi_{m_1, m_2}(x_1, x_2) = \sqrt{\frac{2}{a_1}} \sin\left(\frac{\pi}{a_1} m_1 x_1\right) \sqrt{\frac{2}{a_2}} \sin\left(\frac{\pi}{a_2} m_2 x_2\right). \quad (5)$$

Taking the expansion (4) and substituting into the TISWE (1), we get

$$\hat{H} \sum_m c_m \phi_m(\mathbf{r}) = \left[-\frac{\hbar^2}{2M} \nabla^2 + V'(\mathbf{r})\right] \sum_m c_m \phi_m(\mathbf{r}) = E_n \sum_m c_m \phi_m(\mathbf{r}), \quad (6)$$

with the new potential $V'(\mathbf{r})$ introduced. Next, we multiply through by $\phi_n(\mathbf{r})$ on the left, giving us

$$\phi_n(\mathbf{r}) \left[-\frac{\hbar^2}{2M} \nabla^2 + V'(\mathbf{r})\right] \sum_m c_m \phi_m(\mathbf{r}) = \phi_n(\mathbf{r}) E_n \sum_m c_m \phi_m(\mathbf{r}), \quad (7)$$

which we integrate with respect to \mathbf{r} . To do this, we must make a few preliminary steps. First, we consider the requirement of the basis vectors of a quantum system to be orthonormal. This orthonormality condition can be represented by

$$\int d\mathbf{r} \phi_n(\mathbf{r}) \phi_m(\mathbf{r}) = \delta_{nm} \quad (8)$$

while the Hamiltonian matrix is given by

$$H_{nm} = \int d\mathbf{r} \phi_n(\mathbf{r}) \hat{H} \phi_m(\mathbf{r}). \quad (9)$$

This can be evaluated to give

$$H_{nm} = \frac{\pi^2 \hbar^2}{2m} \left[\left(\frac{m_1}{a_1} \right)^2 + \left(\frac{m_2}{a_2} \right)^2 \right] \delta_{nm} + V_0 v_{nm}, \quad (10)$$

where

$$v_{nm} = \int_{\Gamma'} d^2\mathbf{r} \phi_n(\mathbf{r}) \phi_m(\mathbf{r}). \quad (11)$$

The integral v_{nm} must be computed over the region with potential V_0 . With this final piece of the puzzle, we can take the integral of (7) to be the simple eigenvalue problem

$$\sum_m (H_{nm} - E \delta_{nm}) c_m = 0. \quad (12)$$

The allowed energy levels are then those which satisfy the condition

$$\det|H_{nm} - E \delta_{nm}| = 0. \quad (13)$$

These equations allow us to approximate the discrete energy levels E_n of the system, as well as the values of the wavefunction in the region enclosed by Γ . It is important to note that one must choose a maximum number of expansion terms M_0 to include in the computation. This will determine the size of the Hamiltonian matrix H_{nm} , and consequently the number of eigenvalues that can be obtained.

III. ALGORITHM AND PROGRAM

The method above was applied to the integrable circle system, as well as the non-integrable (chaotic) stadium in MATHEMATICA 8.0. The two goals of the program were to successfully compute the eigenvalues of each system, and to compute and display a density plot of the associated wavefunctions $\psi(\mathbf{r})$. The actual program implemented will be explained step by step, taking care to illustrate the differences between the circle and the stadium.

First, we must designate good parameters M_0 (the number of expansion terms) and V_0 (the potential in region Γ'). Because computation time increases exponentially as M_0 increases, it is easiest to start it low and increase it depending on the number of eigenvalues desired. I recommend beginning with only three expansion terms for either geometry. For the circle, a V_0 value of 50,000 worked well, while the stadium worked better with 100,000. Of course, for either of these, the accuracy of the method would only be increased with higher values. Kaufman, Kosztin, and Schulten recommend letting $\hbar^2/2Ma_1^2 = 1$ to simplify the energy units. The final parameters to consider are the lengths of the rectangle

that encloses Γ' , (a_1, a_2) . It is easiest to center both the circle and the stadium at the origin. Giving the circle a radius of one means that both a_1 and a_2 will be two. For the stadium, I allowed the vertical component a_2 to be two, while the horizontal component a_1 can be anything greater than two.

The next step is to calculate the integral v_{nm} . This is a double integral over both x_1 and x_2 , but because of its computational complexity it is best to break this step into two integrals instead. These integrals should be computed analytically if possible, as numeric integration might result in large errors because of the highly oscillatory nature of the functions. For both the stadium and the circle, I computed the integral over x_2 analytically, but the integral over x_1 had to be done numerically. To reduce error, it is best to choose a working precision, precision goal, and accuracy goal. In MATHEMATICA, I was able to eliminate errors from this integral by requesting a working precision of 30 decimal places and a precision goal of 20 decimal places.

For the circle, the analytic integral over x_2 had to be broken up into two pieces, a top and a bottom:

$$v_{x_2, top} = \int_{\sqrt{1-x_1^2}}^1 \phi_m(\mathbf{r})\phi_n(\mathbf{r}), \quad (14)$$

$$v_{x_2, bottom} = \int_{-1}^{\sqrt{1-x_1^2}} \phi_m(\mathbf{r})\phi_n(\mathbf{r}). \quad (15)$$

The same can be done for the stadium, only now four integrals need to be done, one for each corner of the rectangle. In this case, the bounds of the integral depend explicitly on the side length a_1 that the user has chosen:

$$v_{x_2, topleft} = \int_{\sqrt{1-(x_1+(\frac{a_1}{2}-1))^2}}^1 \phi_m(\mathbf{r})\phi_n(\mathbf{r}), \quad (16)$$

$$v_{x_2, topright} = \int_{\sqrt{1-(x_1-(\frac{a_1}{2}-1))^2}}^1 \phi_m(\mathbf{r})\phi_n(\mathbf{r}), \quad (17)$$

$$v_{x_2, bottomleft} = \int_{-1}^{-\sqrt{1-(x_1+(\frac{a_1}{2}-1))^2}} \phi_m(\mathbf{r})\phi_n(\mathbf{r}), \quad (18)$$

$$v_{x_2, bottomright} = \int_{-1}^{-\sqrt{1-(x_1-(\frac{a_1}{2}-1))^2}} \phi_m(\mathbf{r})\phi_n(\mathbf{r}). \quad (19)$$

It's important to get these bounds right. We want to make sure to integrate over the region where the potential is V_0 , not in the actual billiard region. There might be a discontinuity in the evaluation of the integral at $n_2 = m_2$. If this is the case, MATHEMATICA should be able to take the limit at this point, and you can manually add it into the value for v_{x_2} . The next step is to numerically

calculate v_{x_1} . In this case the bounds are simply the bounds of the rectangle, and the integrand is simply the solution to the x_2 component of v_{nm} . Computing this integral gives us the final v_{nm} needed.

Now that v_{nm} has been calculated, we use (10) to calculate the Hamiltonian matrix H_{nm} . In this calculation n_1, n_2, m_1 , and m_2 should all run from one to M_0 . The term δ_{nm} is the product $\delta_{m_1, n_1} \delta_{m_2, n_2}$. We are now prepared to compute the energy eigenvalues of the system. MATHEMATICA conveniently has an 'eigenvalues' function. The eigenvalues that it returns should be sorted from lowest to highest for proper analysis, and have units of $\hbar^2/2Ma_1^2$. The higher eigenvalues are less likely to be accurate, and so may be discarded. Nonetheless, the lower ones should approximate the actual energy levels closely. Solutions to the TISWE for a circular infinite potential well are well known Bessel functions, so checking for accuracy of the method should be simple. When the energy eigenvalues have been properly calculated, one can consider increasing the number of expansion terms. There are M_0^2 eigenvalues for a given M_0 that can be returned. A good energy level analysis could use thousands of eigenvalues, although this would require lengthy computation. Computing and ordering the eigenvectors is just as easily accomplished, and correspond to the expansion coefficients c_m .

The final step in the program is actually computing the eigenfunctions $\psi_n(\mathbf{r})$ using the original expansion (4). The probability density is given by

$$|\psi_n(\mathbf{r})|^2 = \psi_n(\mathbf{r})\psi_n(\mathbf{r}). \quad (20)$$

Doing a plot of this density with a grayscale should give good images of the solutions to the wave equation for the geometries in question. MATHEMATICA allows us to draw on top of our plots using the 'epilog' function, so we can outline the boundaries we were concerned with from the beginning (the circle and the stadium).

IV. PLOTS & ENERGY LEVELS

Figures 2 and 3 show a log plot of the eigenvalues of the $n \times m$ Hamiltonian matrix for the circle billiard and the stadium billiard respectively. The circle billiards have 81 eigenvalues while the stadium has 100 (each has the square of the number of expansion terms M_0). One may notice that the energy levels shoot up exponentially after a certain point. There are methods to test the accuracy of the eigenvalues computed, although they have not been used here. One such method involves using a transformation to linearly scale the energies and then testing their agreement with a Weyl-formula, such as

$$\langle N(E) \rangle = \frac{1}{4\pi} (AE - L\sqrt{E} + C) \quad (21)$$

where A and L are the area and perimeter of the billiard, and C is a topological constant [5]. I have neglected such

a test, although it should be done if time is available. I decided to toss the higher energy levels given due to suspicion about mounting error. Figures 4 and 5 show a selection of density plots of the wavefunctions $|\psi_n|$ for each of the systems. The first nine eigenfunctions are shown for the circle, while nine increasing but not continuous eigenfunctions were chosen for the stadium.

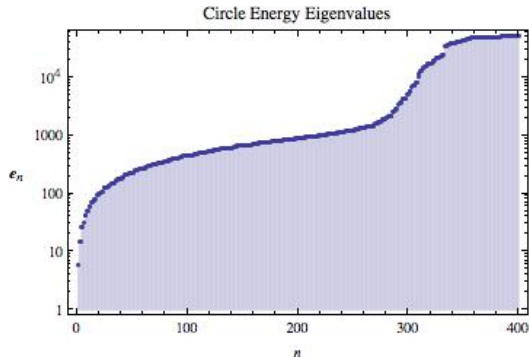


FIG. 2: List of eigenvalues for the circle system, generated using twenty expansion terms. The higher eigenvalues ($n > 250$) may have been subject to larger numerical roundoff errors, and can be discounted from analysis.

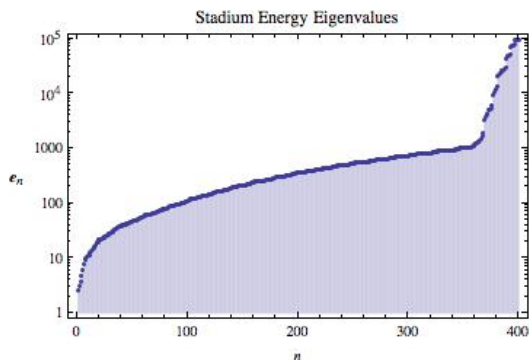


FIG. 3: List of eigenvalues for the stadium system, generated using twenty expansion terms. Like the circle system, only the lower eigenvalues ($n < 350$) may be trusted in analysis.

V. PRELIMINARY ENERGY SPACING ANALYSIS AND FUTURE WORK

Because quantum mechanical systems do not have phase spaces which can display extreme sensitivity to initial conditions (as classical systems do), analogues to classical chaos are sought in the spacing of the energy levels. The energy levels are given by the eigenvalues of the Hamiltonian matrix H_{nm} . One common way to analyze energy level spacings is through a nearest neighbor plot. If we have n useable energy levels, then we can examine the spacing between subsequent levels by plotting a normalized histogram of $E_{n+1} - E_n$ about some spacing

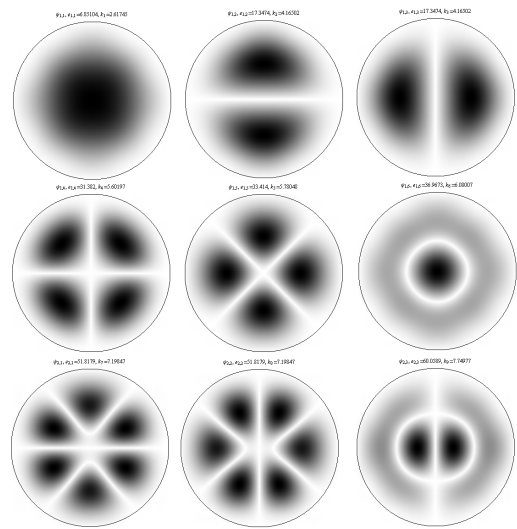


FIG. 4: The first nine eigenfunctions of the infinite circular well. These solutions represent the classic bessel functions which have historically been used to solve the Helmholtz equation.

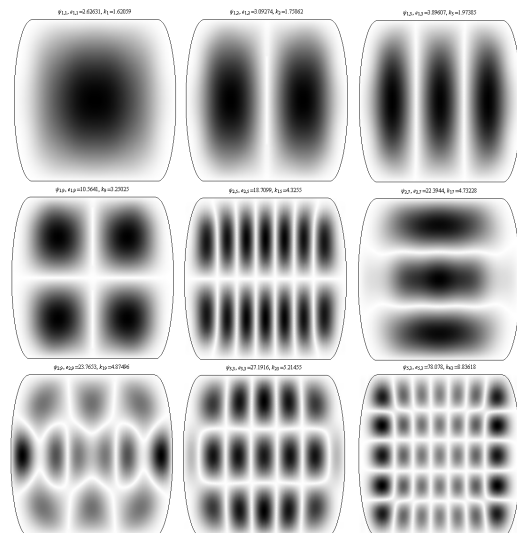


FIG. 5: A mixed assortment of eigenfunctions from the stadium with horizontal extension $a_1 = 8.88$, with aspect ratio set to one.

ds :

$$\int P(s)ds = \sum_n \frac{E_{n+1} - E_n}{n} = 1. \quad (22)$$

The difference between integrable systems (like the circle) and nonintegrable systems (like the stadium) is that an integrable system has the same number of constants of motion as its dimension, whereas a nonintegrable system has fewer constants of motion than its dimension (though that distinction has been contested [6]). According to Random Matrix Theory, a classically integrable system

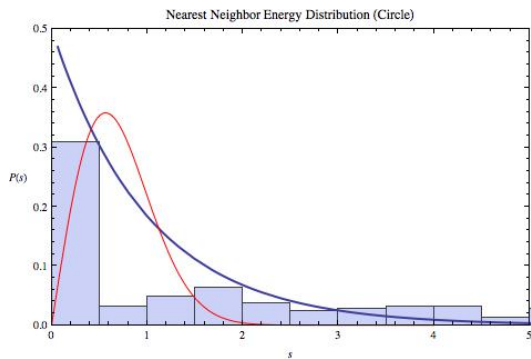


FIG. 6: Nearest Neighbor energy spacings for the circle billiard. The blue line is the Poisson distribution, while the red line is the Gaussian Orthogonal Ensemble.

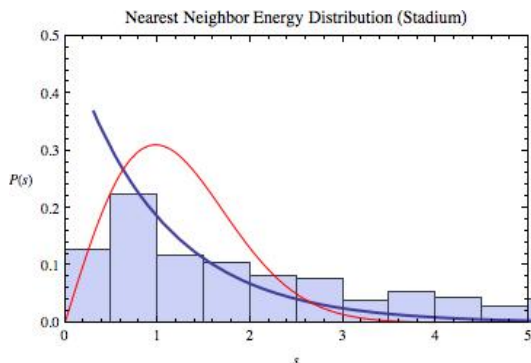


FIG. 7: Nearest Neighbor energy spacings for the stadium billiard. The blue line is the Poisson distribution, while the red line is the Gaussian Orthogonal Ensemble

should have an energy level spacing that can be fit by a Poisson distribution,

$$P_0(s) = e^{-s}, \quad (23)$$

while a classically chaotic system should be better fit by a Gaussian Orthogonal Ensemble [7],

$$P_{GOE}(s) = \frac{\pi}{2} s \exp\left(-\frac{\pi s^2}{4}\right). \quad (24)$$

Figures 6 and 7 show nearest neighbor histograms for each of the two systems examined. Each has a GOE and Poisson distribution superimposed on them (red and blue respectively). We can at least intuitively see that the Poisson distribution fits the circle histogram better, while the GOE fits the stadium better - each fitting their analogous classical counterparts. Unfortunately, a clearer analysis of this data isn't possible without more eigenvalues. The range of eigenvalues used to analyze energy level spacing ranges from a few hundred to many thousands. Nonetheless, I think the figures can help one believe that the stadium billiard shares characteristics with classical chaotic systems, while the circle billiard shares characteristics with classical integrable systems.

There are many paths a quantum billiard project could pursue. To study the chaotic properties of nonintegrable systems like the stadium billiard in detail, more eigenvalues need to be calculated. Those eigenvalues then need to be tested for accuracy before their spacing is analyzed. A better fit of the GOE distribution should be done, and how well it fits should be represented numerically. Other nonintegrable systems could be studied, such as the general triangle or the Sinai billiard [5]. Another option would be to focus on applications such as the modelling of nanodevices, rather than only studying theoretical properties of the systems[8]. The analogous Helmholtz equation allows researchers to use experimental techniques to test the results of 2-D quantum billiard simulations[9]. The project could be extended in any of these directions and perhaps further.

-
- [1] Serway, Moses, Moyer, *Modern Physics*, Instructor's Ed. (Saunders College, New York, 1989), pg. 194-212.
 - [2] W. T. Lu, W. Zeng, and S. Sridhar, "Duality between quantum and classical dynamics for integrable billiards," *Phys. Rev. E* 73, 1-11 (2006).
 - [3] O. Bengtsson, J. Larsson, and K. F. Berggren, "Emulation of quantum mechanical billiards by electrical resonance circuits," *Phys. Rev. E* 71, 1-11 (2005).
 - [4] A. Kudrolli, S. Sridhar, A. Pandey, and R. Ramaswamy, "Signatures of chaos in quantum billiards: microwave experiments," *Phys. Rev. E* 49, 11-14 (1993).
 - [5] D. L. Kaufman, I. Kosztin and K. Schulten, "Expansion method for stationary states of quantum billiards," *Am. J. Phys.* 67, 133-141 (1998).
 - [6] W. Zhang, D. H. Feng, and J. Yuan, "Integrability and nonintegrability of quantum systems: Quantum integrability and dynamical symmetry," *Phys. Rev. A* 40, 438-447 (1989).
 - [7] D. Delande and J. C. Gay, "Quantum chaos and statistical properties of energy levels: numerical study of the hydrogen atom in a magnetic field," *Phys. Rev. Lett.* 57, 1-4 (1986).
 - [8] F. Miao, S. Wijeratne, Y. Zhang, U. C. Coskun, W. Bao, and C. N. Lau, "Phase coherent transport in graphene quantum billiards," *Science* 317, 1530-1533.
 - [9] N. Burq and M. Zworski, "Bouncing Ball Modes and Quantum Chaos," *SIAM Rev.* 47, 43-49 (2005).